UNIVERSITI PUTRA MALAYSIA

EFFECTS OF Pr6O11 ADDITION AND SINTERING TEMPERATURE ON STRUCTURAL, OPTICAL AND LUMINESCENCE PROPERTIES OF Zn2SiO4 BASED GLASS CERAMICS

NURZILLA BINTI MOHAMED

FS 2018 3

EFFECTS OF Pr_6O_{11} ADDITION AND SINTERING TEMPERATURE ON STRUCTURAL, OPTICAL AND LUMINESCENCE PROPERTIES OF Zn_2SiO_4 BASED GLASS CERAMICS

By

NURZILLA BINTI MOHAMED

Thesis Submitted to the School of Graduate Studies, Universiti Putra Malaysia, in Fulfilment of the Requirement for the Degree of Doctor of Philosophy

December 2017

© COPYRIGHT UPM

COPYRIGHT

All material contained within the thesis, including without limitation text, logos, icons, photographs and all other artwork, is copyright material of Universiti Putra Malaysia unless otherwise stated. Use may be made of any material contained within the thesis for non-commercial purposes from the copyright holder. Commercial use of material may only be made with the express, prior, written permission of Universiti Putra Malaysia.

Copyright © Universiti Putra Malaysia

© COPYRIGHT UPM

In appreciation of their love and sacrifices, this thesis is dedicated to my family especially my beloved parents MOHAMED B. SALLEH and CHE HASNA@RAHMAH BT AHMAD and my siblings who have been giving me full moral support throughout the years.

© COPYRIGHT UPM

Abstract of thesis presented to the Senate of Universiti Putra Malaysia in fulfilment of the requirement for the degree of Doctor of Philosophy

EFFECTS OF Pr_6O_{11} ADDITION AND SINTERING TEMPERATURE ON STRUCTURAL, OPTICAL AND LUMINESCENCE PROPERTIES OF Zn_2SiO_4 BASED GLASS CERAMICS

By

NURZILLA BINTI MOHAMED

December 2017

Chairman: **Associate Professor Jumiah Hassan, PhD**
Faculty: **Science**

In recent years, great interest was focused on glass ceramics for applications in laser, optical amplifier and optical sensor. Up to now, the commercial Zn_2SiO_4 were fabricated due to its high luminescence and chemical stability. This research highlights the alternative sources of SLS-ZnO glass in order to produce Zn_2SiO_4 glass ceramics by varying Pr concentration and sintering temperatures. The six series of Pr addition into SLS-ZnO glasses of the type $_x(Pr_6O_{11})._{100-x}(SLS_{0.5}\text{-}ZnO_{0.5})$ (where x = 0, 1, 2, 3, 4, at 5 wt. %) were prepared by mixing the raw materials Praseodymium Oxide (Pr_6O_{11}), Soda Lime Silica (SLS)and Zinc Oxide (ZnO) as starting materials in the appropriate amount. Then, these mixture materials were melted at 1400 ^oC for 2 hours in alumina crucibles by electrical furnace. The molten glass was poured into water by quenching technique in order to produce glass frit. The glass fritz was finely ground and sieved to be in powder form with the size of 63 µm. Density of SLS-ZnO glass increases by increasing Pr concentration. The glass system which consists of amorphous phase and more non-bridging oxygen were confirmed by XRD and FTIR analysis. The band gap fluctuated when Pr concentration is lower than 3 wt.% and enhanced at higher Pr concentration (4 and 5 wt.%). However, the luminescence intensity decreased as the Pr concentration increased from 4 to 5 wt.% may due to the concentration quenching effects.

Besides that, Pr doped Zn_2SiO_4 glass ceramics were prepared by sintering SLS-ZnO glass from 600 to 1000 ^oC. The properties of Pr addition into Zn_2SiO_4 were evaluated in terms of structural, optical and luminescence properties at different sintering temperatures. The formation of α-Zn_2SiO_4 in the SLS-ZnO host matrix is proven by XRD, FTIR, FESEM and EDX analysis. The XRD indicates the peaks of α-Zn_2SiO_4 increases in intensity with increasing sintering temperatures by increasing Pr concentration from 0 to 2 wt.% Pr. Nevertheless, the intensity of α-Zn_2SiO_4 phase decreases at 3 wt.% Pr but increases at high Pr concentration (4 and 5 wt.% Pr). The

© COPYRIGHT UPM

FTIR spectra showed the presence of Zn_2SiO_4 phase in the glass ceramics network occurring at ~467 and ~697 cm^{-1} which is supported by EDX analysis. FESEM micrographs showed the grain growth increases with increasing sintering temperatures. The average grain growth decreases as Pr concentration increases from 1 to 5 wt.%. The sharpness absorption band of ~444 nm increases as Pr concentration and sintering temperatures increases which is in good agreement with the excitation of blue LED for the fabrication of White Light Emitting Diode (WLED).

The band gap increases with increasing sintering temperatures up to 900 ^oC and decreases with further sintering of 1000 ^oC due to the crystallinity of Zn_2SiO_4 phase. The substitution of Pr addition into the host matrix fluctuates the band gap when Pr concentration is lower than 4 wt.% and decreases at 5 wt.% Pr. The increase in crystallinity of Zn_2SiO_4 is suggested to be due to the enhancement of the luminescence with increasing sintering temperatures. It is interesting to note that the luminescence intensity decreases by increasing Pr concentration up to 3 wt.% to increase at 4 and 5 wt.% Pr due to the incorporation of the Pr^{3+} ion in the Zn_2SiO_4. This suggests that Pr doped Zn_2SiO_4 possess suitable structural, optical and luminescence properties and could be a promising glass ceramic material for optoelectronics devices.

© COPYRIGHT UPM

Abstrak tesis yang dikemukakan kepada Senat Universiti Putra Malaysia sebagai memenuhi keperluan untuk Ijazah Doktor Falsafah

KESAN PENAMBAHAN Pr_6O_{11} DAN SUHU PENSINTERAN PADA SIFAT STRUKTUR, OPTIK DAN KEPENDARKILAUAN Zn_2SiO_4 BERASASKAN KACA SERAMIK

Oleh

NURZILLA BINTI MOHAMED

Disember 2017

Pengerusi: **Prof. Madya Jumiah Hassan, PhD**
Fakulti: **Sains**

Sejak kebelakangan ini, minat yang tinggi telah difokuskan pada seramik kaca untuk aplikasi dalam laser, penguat optik dan sensor optik. Sehingga kini, komersial Zn_2SiO_4 telah direka kerana kependarkilauan tinggi dan kestabilan kimia. Kajian ini menekankan sumber alternatif kaca SLS-ZnO untuk menghasilkan seramik kaca Zn_2SiO_4 dengan pelbagai kepekatan Pr dan suhu pensinteran. Enam siri penambahan Pr kepada kaca SLS-ZnO dari jenis $_x(Pr_6O_{11}).\ _{100-x}(SLS_{0.5}\text{-}ZnO_{0.5})$ (di mana x = 0, 1, 2, 3, 4, pada 5 wt.%) telah disediakan dengan mencampurkan bahan-bahan mentah Praseodymium Oxide (Pr_6O_{11}), Soda Lime Silica (SLS) dan Zinc Oxide (ZnO) sebagai bahan permulaan dalam jumlah yang sesuai. Kemudian, bahan campuran ini dicairkan pada 1400 ^oC selama 2 jam di dalam mangkuk pijar alumina oleh relau elektrik. Kaca cecair dituangkan ke dalam air dengan teknik lindapan untuk menghasilkan fritz kaca. Fritz kaca itu dikisar dengan halus dan ditapis menjadi bentuk serbuk dengan saiz 63 μm. Ketumpatan kaca SLS-ZnO meningkat dengan peningkatan kepekatan Pr. Sistem kaca yang terdiri daripada fasa amorfus dan lebih banyak oksigen bukan penyambungan (NBO) telah disahkan oleh analisisa XRD dan FTIR. Jurang band turun naik apabila kepekatan Pr lebih rendah daripada 3 wt.% dan dipertingkatkan pada kepekatan Pr yang lebih tinggi (4 dan 5 wt.%). Walau bagaimanapun, keamatan keperdakilauan menurun apabila kepekatan Pr meningkat dari 4 wt.% hingga 5 wt.% mungkin disebabkan oleh kesan kepekatan pelindapkejutan.

Selain itu, seramik kaca Zn_2SiO_4 telah disediakan melalui pensinteran SLS-ZnO kaca dari 600 hingga 1000 ^oC. Pencirian penambahan Pr di dalam Zn_2SiO_4 sampel dinilai dari segi struktur, optik dan kependarkilauan pada suhu pensinteran yang berbeza. Pembentukan α-Zn_2SiO_4 dalam matriks SLS- ZnO dibuktikan oleh analisisa XRD, FTIR, FESEM dan EDX. XRD menunjukkan bahawa puncak keamatan α-Zn_2SiO_4 meningkat dengan peningkatan suhu pensinteran. Keamatan fasa α-Zn_2SiO_4 meningkat dengan meningkatkan kepekatan Pr dari 0 hingga 2 wt.% Pr. Walau

© COPYRIGHT UPM

bagaimanapun, keamatan fasa α-Zn_2SiO_4 telah menurun pada 3 wt.% Pr dan meningkat pada kepekatan Pr tertinggi (4 dan 5 wt.% Pr). Spektrum FTIR menunjukkan kehadiran fasa Zn_2SiO_4 dalam rangkaian seramik kaca berlaku pada ~467 dan ~697 cm^{-1} yang disokong oleh analisisa EDX. Mikrograf FESEM menunjukkan pertumbuhan butiran meningkat dengan peningkatan suhu pensinteran. Purata pertumbuhan butiran menurun apabila kepekatan Pr meningkat dari 1 hingga 5 wt.%. Ketajaman jalur penyerapan pada ~444 nm telah meningkat apabila kepekatan Pr dan suhu pensinteran meningkat yang dipersetujui dengan pengujaan LED biru untuk fabrikasi Diode Pemancar Cahaya Putih (WLED).

Jurang jalur meningkat dengan peningkatan suhu pensinteran hingga 900 ^oC dan berkurang dengan pensinteran lebih lanjut pada 1000 ^oC disebabkan oleh kekristalan fasa Zn_2SiO_4. Penggantian penambahan Pr ke dalam matriks tuan rumah akan turun naik dalam jurang jalur apabila kepekatan Pr lebih rendah daripada 4 wt.% dan berkurangan pada 5 wt.% Pr. Peningkatan kekristalan Zn_2SiO_4 disarankan untuk mempertingkatkan kependarkilauan dengan peningkatan suhu pensinteran. Adalah menarik untuk diperhatikan bahawa keamatan keperdakilauan berkurang dengan peningkatan kepekatan Pr hingga 3 wt.% dan kemudian mula meningkat pada 4 dan 5 wt.% Pr disebabkan oleh penggabungan ion Pr^{3+} dalam Zn_2SiO_4. Ini menunjukkan bahawa penambahan Pr di dalam Zn_2SiO_4 mempunyai sifat struktur, optik dan kependarkilauan yang sesuai dan boleh menjadi bahan seramik kaca yang menjanjikan untuk peranti optoelektronik.

© COPYRIGHT UPM

ACKNOWLEDGEMENTS

It is neither my strength nor my wisdom, but Allah's mercies that made this work a success, thus, I glorify Him. May all praises and salutations of the Lord be upon the Messenger of Allah and upon his Family and Companions, and those who are guided by the light of his 'sunnah' till the Day of Judgment.

I would first like to thank Assoc. Prof. Dr. Jumiah Hassan as my supervisor at Faculty of Science who guided me throughout my research. I would also like to extent my sincere thanks to Dr. Zaidan Abdul Wahab, Dr. Khamirul Amin Matori and Dr. Raba'ah Syahidah Azis.

Others I would like to thank to my lab mates in the Ceramic Composite Glass Material. I really appreciate their discussions, ideas, memorable interactions and time spent throughout this research. To my fellow friends, Fadzidah, Rahimah, Hapishah, Idza, Nur Fadilah, Zamratul, Zarifah, Ain, Hanim and many others I want to say thanks for everything. I would also like to express my appreciation to all Faculty of Science staff and ITMA staff for their great helps and contributions to my thesis work.

Finally, I am highly grateful for the love, care, prayer and support from my beloved parents Mohamed b. Salleh and Che Hasna@Rahmah bt Ahmad and my siblings Dzulkifli, Asnazalia, Zuraida, Kamsiah and Rozaili with honest supporting me to complete this work successfully.

© COPYRIGHT UPM

I certify that a Thesis Examination Committee has met on 14 December 2017 to conduct the final examination of Nurzilla binti Mohamed on her thesis entitled "Effects of Pr_6O_{11} Addition and Sintering Temperature on Structural, Optical and Luminescence Properties of Zn_2SiO_4 Based Glass Ceramics" in accordance with the Universities and University Colleges Act 1971 and the Constitution of the Universiti Putra Malaysia [P.U.(A) 106] 15 March 1998. The Committee recommends that the student be awarded the Doctor of Philosophy.

Members of the Thesis Examination Committee were as follows:

Zulkifly bin Abbas, PhD
Associate Professor
Faculty of Science
Universiti Putra Malaysia
(Chairman)

Abdul Halim bin Shaari, PhD
Professor
Faculty of Science
Universiti Putra Malaysia
(Internal Examiner)

Hishamuddin bin Zainuddin, PhD
Associate Professor
Faculty of Science
Universiti Putra Malaysia
(Internal Examiner)

Raouf Abdle Hamid El-Mallawany, PhD
Professor
Menofia University
Egypt
(External Examiner)

NOR AINI AB. SHUKOR, PhD
Professor and Deputy Dean
School of Graduate Studies
Universiti Putra Malaysia

Date: 27 February 2018

This thesis was submitted to the Senate of Universiti Putra Malaysia and has been accepted as fulfilment of the requirement for the degree of Doctor of Philosophy. The members of the Supervisory Committee were as follows:

Jumiah Hassan, PhD
Associate Professor
Faculty of Science
Universiti Putra Malaysia
(Chairman)

Khamirul Amin Matori, PhD
Associate Professor
Faculty of Science
Universiti Putra Malaysia
(Member)

Raba'ah Syahidah Azis, PhD
Senior lecturer
Faculty of Science
Universiti Putra Malaysia
(Member)

_____
ROBIAH BINTI YUNUS, PhD
Professor and Dean
School of Graduate Studies
Universiti Putra Malaysia

Date:

© COPYRIGHT UPM

Declaration by graduate student

I hereby confirm that:

- this thesis is my original work;
- quotations, illustrations and citations have been duly referenced;
- this thesis has not been submitted previously or concurrently for any other degree at any other institutions;
- intellectual property from the thesis and copyright of thesis are fully-owned by Universiti Putra Malaysia, as according to the Universiti Putra Malaysia (Research) Rules 2012;
- written permission must be obtained from supervisor and the office of Deputy Vice-Chancellor (Research and Innovation) before thesis is published (in the form of written, printed or in electronic form) including books, journals, modules, proceedings, popular writings, seminar papers, manuscripts, posters, reports, lecture notes, learning modules or any other materials as stated in the Universiti Putra Malaysia (Research) Rules 2012;
- there is no plagiarism or data falsification/fabrication in the thesis, and scholarly integrity is upheld as according to the Universiti Putra Malaysia (Graduate Studies) Rules 2003 (Revision 2012-2013) and the Universiti Putra Malaysia (Research) Rules 2012. The thesis has undergone plagiarism detection software.

Signature: _____ Date: _____

Name and Matric No.: Nurzilla Binti Mohamed (GS40976)

© COPYRIGHT UPM

Declaration by Members of Supervisory Committee

This is to confirm that:

- the research conducted and the writing of this thesis was under our supervision;
- supervision responsibilities as stated in the Universiti Putra Malaysia (Graduate Studies) Rules 2003 (Revision 2012-2013) are adhered to

Signature: _____
Name of Chairman
of Supervisory
Committee: _____

Signature: _____
Name of Member
of Supervisory
Committee: _____

Signature: _____
Name of Member
of Supervisory
Committee: _____

© COPYRIGHT UPM

TABLE OF CONTENTS

		Page
ABSTRACT		i
ABSTRAK		iii
ACKNOWLEDGEMENTS		v
APPROVAL		vi
DECLARATION		viii
LIST OF TABLES		xiii
LIST OF FIGURES		xiv
LIST OF ABBREVIATIONS AND SYMBOLS		xxi
CHAPTER		
1 INTRODUCTION		
1.1	Background of study	1
1.2	Phase formation of willemite	2
1.3	Significant and motivation of research	4
1.4	Problem statements	4
1.5	Objectives	5
1.5.1	Main research project objective	5
1.5.2	Work phase objectives	5
1.6	Hypothesis	5
1.7	Thesis outline	6
2 LITERATURE REVIEW		
2.1	Introduction	7
2.2	Glass system	7
2.2.1	Soda lime silica (SLS)	8
2.3	Glass ceramics system	9
2.4	Zinc oxide	10
2.5	Praseodymium oxide	10
2.6	Density	11
2.7	Thermal properties	12
2.8	Structural	12
2.8.1	XRD	12
2.8.2	FTIR	13
2.8.3	FESEM	14
2.9	Optical	15
2.9.1	Absorption	15
2.9.2	Optical band gap	16
2.10	Luminescence	17
3 THEORY		
3.1	Introduction	22
3.2	Process of glass ceramics	22
3.3	Mechanism of absorption	23
3.3.1	Addition effect on band gap	25

© COPYRIGHT UPM

3.4 Mechanism of luminescence 26
3.4.1 Luminescence phenomena of phosphor 27
3.4.2 Mechanism of energy transfer in rare earth phosphor 28
3.4.3 Concept of luminescence by band gap theory 28

4 METHODOLOGY
4.1 Introduction 30
4.2 Raw materials 31
4.3 Milling process 32
4.4 Melting and quenching 32
4.5 Pellet preparation 33
4.6 Heat treatment (sintering) 33
4.7 Material characteristics measurements 34
4.7.1 Density 34
4.7.2 Differential Scanning Calorimetry (DSC) 34
4.7.3 X-ray Diffraction (XRD) 35
4.7.4 Fourier Transform Infrared Spectroscopy (FTIR) 36
4.7.5 Field Emission Scanning Electron Microscopy (FESEM) 37
4.7.6 Energy Dispersive X-ray Spectroscopy (EDX) 38
4.7.7 UV-Visible spectrometers 39
4.7.8 Photoluminescence spectrometer 40

5 RESULTS AND DISCUSSION
5.1 Introduction 42
5.2 Density 42
5.2.1 Pr addition in SLS-ZnO glass 42
5.2.2 Pr addition in SLS-ZnO glass ceramics 43
5.3 Thermal analysis 44
5.4 Structural 46
5.4.1 XRD 46
5.4.1.1 Raw materials 46
5.4.1.2 Pr addition in SLS-ZnO glass 48
5.4.1.3 Pr addition in SLS-ZnO glass ceramics 48
5.4.1.4 Various Pr concentration 55
5.4.2 FTIR 60
5.4.2.1 Pr addition in SLS-ZnO glass 60
5.4.2.2 Pr addition in SLS-ZnO glass ceramics 62
5.4.2.3 Various Pr concentrations 68
5.4.3 FESEM 74
5.4.3.1 Undoped glass ceramics 74

© COPYRIGHT UPM

5.4.3.2 Pr addition in SLS-ZnO glass ceramics 76
5.4.3.3 Grain size distribution 83
5.4.3.4 EDX of starting materials 90
5.4.3.5 EDX of undoped glass ceramics 91
5.4.3.6 EDX of Pr addition in SLS-ZnO Glass ceramics 93
5.5 Optical 106
5.5.1 Absorption spectra 106
5.5.1.1 Pr addition in SLS-ZnO glass 106
5.5.1.2 Pr addition in SLS-ZnO glass ceramics 107
5.5.1.3 Various Pr concentrations 111
5.5.2 Band gap 115
5.5.2.1 Pr addition in SLS-ZnO glass 115
5.5.2.2 Pr addition in SLS-ZnO glass ceramics 118
5.5.2.3 Various Pr concentrations 131
5.6 Luminescence Analysis 136
5.6.1 Pr addition in SLS-ZnO glass 136
5.6.2 Pr addition in SLS-ZnO glass ceramics 138
5.6.3 Various Pr concentrations 142
5.6.4 Energy level of Pr addition 145

6 CONCLUSION AND RECOMMENDATIONS
6.1 Conclusion 147
6.2 Recommendations for Future Work 148

REFERENCES 149
BIODATA OF STUDENT 163
LIST OF PUBLICATIONS 164

© COPYRIGHT UPM

LIST OF TABLES

Table		Page
2.1	Summary on important parameters of the glass and glass ceramics system	19
4.1	Chemical composition of Pr addition in SLS-ZnO glass	32
5.1	Glass transition temperature, Tg, temperature of crystallization, Tc and thermal stability range ΔT of Pr addition in SLS-ZnO glass	45
5.2	FTIR wavenumber and vibrational mode of Pr addition in SLS-ZnO glass	62
5.3	FTIR wavenumber and vibrational mode of Pr addition in SLS-ZnO glass ceramics	73
5.4	Grain size of various Pr concentration at 700, 800, 900 and 1000 ^{o}C	82
5.5	Variation of optical band gap of Pr addition in SLS-ZnO glass	117
5.6	Variation of optical band gap of 0 wt.% Pr at 600, 700, 800, 900 and 1000 ^{o}C	120
5.7	Variation of optical band gap of 1 wt.% Pr at 600, 700, 800, 900 and 1000 ^{o}C	127
5.8	Variation of optical band gap of 2 wt.% Pr at 600, 700, 800, 900 and 1000 ^{o}C	127
5.9	Variation of optical band gap of 3 wt.% Pr at 600, 700, 800, 900 and 1000 ^{o}C	127
5.10	Variation of optical band gap of 4 wt.% Pr at 600, 700, 800, 900 and 1000 ^{o}C	128
5.11	Variation of optical band gap of 5 wt.% Pr at 600, 700, 800, 900 and 1000 ^{o}C	128

© COPYRIGHT UPM

LIST OF FIGURES

Figure		Page
1.1	Equilibrium phase diagram for ZnO-SiO_2 system	3
1.2	Crystalline structure of α phase Zn_2SiO_4	3
2.1	Schematic of two- dimensional illustration of the atomic arrangement in glass	7
3.1	Schematic diagram of charge carrier on the lowest energy transition from the valence band to conduction bands where (a) is the band gap of undoped (b) is the Burstein Moss shift and (c) represents band gap renomalization	26
3.2	Schematic diagram of luminescence mechanism where A is called as activator	27
3.3	Schematic diagram of Configurational Coordinate Model (CCM)	28
3.4	The schematic energy band diagram of Pr^{3+} energy level in host matrix energy band gap	29
4.1	Flowchart for preparation and characterization of praseodymium doped willemite based glass ceramics	31
4.2	Schematic diagram of the milling process	32
4.3	Schematic diagram of the temperature profile for the sintering of samples	33
4.4	Schematic diagram of Differential Scanning Calorimetry (DSC)	35
4.5	Schematic diagram of X-ray Diffraction (XRD)	36
4.6	Schematic diagram of Fourier transform infrared spectroscopy (FTIR) analysis	37
4.7	Schematic diagram of Field Emission Scanning Electron Microscopy (FESEM)	38
4.8	Components of a modern digital Energy Dispersive Spectroscopy (EDS) system	39
4.9	Schematic diagram of a double beam UV- Vis spectrometer	40

© COPYRIGHT UPM

4.10	Schematic diagram of Photoluminescence (PL) spectroscopy	41
5.1	Density of Pr addition in SLS-ZnO glass	43
5.2	Density of Pr addition in SLS-ZnO glass ceramics	44
5.3	DSC patterns of Pr addition in SLS-ZnO glass	45
5.4	XRD of Pr_6O_{11}	46
5.5	XRD of Zinc Oxide (ZnO)	47
5.6	XRD of Soda Lime Silica (SLS)	47
5.7	XRD pattern of Pr addition in SLS-ZnO glass	48
5.8	XRD pattern of 0 wt.%Pr at 600,700,800, 900 and 1000 ^oC	50
5.9	XRD pattern of 1 wt.% Pr at 600,700,800, 900 and 1000 ^oC	51
5.10	XRD pattern of 2 wt.% Pr at 600,700,800, 900 and 1000 ^oC	52
5.11	XRD pattern of 3 wt.% Pr at 600,700,800, 900 and 1000 ^oC	53
5.12	XRD pattern of 4 wt.% Pr at 600,700,800, 900 and 1000 ^oC	54
5.13	XRD pattern of 5 wt.% Pr at 600,700,800, 900 and 1000 ^oC	55
5.14	XRD pattern of various Pr concentration at 600 ^oC	56
5.15	XRD pattern of various Pr concentration at 700 ^oC	57
5.16	XRD pattern of various Pr concentration at 800 ^oC	58
5.17	XRD pattern of various Pr concentration at 900 ^oC	59
5.18	XRD pattern of various Pr concentration at 1000 ^oC	60
5.19	FTIR spectra of Pr addition in SLS-ZnO glass	61

© COPYRIGHT UPM

5.20	FTIR spectra of 0 wt.% Pr at 600,700, 800, 900 and 1000 ^{o}C	63
5.21	FTIR spectra of 1 wt.% Pr at 600,700, 800,900 and 1000 ^{o}C	64
5.22	FTIR spectra of 2 wt.% Pr at 600,700, 800,900 and 1000 ^{o}C	65
5.23	FTIR spectra of 3 wt.% Pr at 600,700, 800,900 and 1000 ^{o}C	66
5.24	FTIR spectra of 4 wt.% Pr at 600,700, 800,900 and 1000 ^{o}C	67
5.25	FTIR spectra of 5 wt.% Pr at 600,700, 800,900 and 1000 ^{o}C	68
5.26	FTIR spectra of various Pr concentration at 600 °C	69
5.27	FTIR spectra of various Pr concentration at 700 ^{o}C	70
5.28	FTIR spectra of various Pr concentration at 800 ^{o}C	71
5.29	FTIR spectra of various Pr concentration at 900 ^{o}C	72
5.30	FTIR spectra of various Pr concentration at 1000 ^{o}C	73
5.31	FESEM micrographs of 0 wt.% Pr: (a) 600 ^{o}C, (b) 700 ^{o}C, (c) 800 ^{o}C, (d) 900 ^{o}C, and (e) 1000 ^{o}C	75
5.32	FESEM micrographs of 1 wt.% Pr: (a) 600 ^{o}C, (b) 700 ^{o}C, (c) 800 ^{o}C, (d) 900 ^{o}C, and (e) 1000 ^{o}C	77
5.33	FESEM micrographs of 2 wt.% Pr: (a) 600 ^{o}C, (b) 700 ^{o}C, (c) 800 ^{o}C, (d) 900 ^{o}C, and (e) 1000 ^{o}C	78
5.34	FESEM micrographs of 3 wt.% Pr: (a) 600 ^{o}C, (b) 700 ^{o}C, (c) 800 ^{o}C, (d) 900 ^{o}C, and (e) 1000 ^{o}C	79
5.35	FESEM micrographs of 4 wt.% Pr: (a) 600 ^{o}C, (b) 700 ^{o}C, (c) 800 ^{o}C, (d) 900 ^{o}C, and (e) 1000 ^{o}C	80
5.36	FESEM micrographs of 5 wt.% Pr: (a) 600 ^{o}C, (b) 700 ^{o}C, (c) 800 ^{o}C, (d) 900 ^{o}C, and (e) 1000 ^{o}C	81

© COPYRIGHT UPM

5.37	Average grain size of various Pr concentration at 600,700,800, 900 and 1000 ^{o}C	82
5.38	Grain size distribution of 0 wt.%Pr at (a) 700 ^{o}C, (b) 800 ^{o}C,(c) 900 ^{o}C and (d) 1000 ^{o}C	84
5.39	Grain size distribution of 1 wt.%Pr at (a) 700 ^{o}C, (b) 800 ^{o}C, (c) 900 ^{o}C and (d) 1000 ^{o}C	85
5.40	Grain size distribution of 2 wt.%Pr at (a) 700 ^{o}C, (b) 800 ^{o}C, (c) 900 ^{o}C and (d) 1000 ^{o}C	86
5.41	Grain size distribution of 3 wt.%Pr at (a) 700 ^{o}C, (b) 800 ^{o}C, (c) 900 ^{o}C and (d) 1000 ^{o}C	87
5.42	Grain size distribution of 4 wt.%Pr at (a) 700 ^{o}C, (b) 800 ^{o}C, (c) 900 ^{o}C and (d) 1000 ^{o}C	88
5.43	Grain size distribution of 5 wt.%Pr at (a) 700 ^{o}C, (b) 800 ^{o}C, (c) 900 ^{o}C and (d) 1000 ^{o}C	89
5.44	EDX analysis of starting materials (a) Pr_6O_{11}, (b) SLS and (c) ZnO	91
5.45	EDX analysis of 0 wt.% Pr: (a) 600 ^{o}C, (b) 700 ^{o}C, (c) 800 ^{o}C, (d) 900 ^{o}C, and (e) 1000 ^{o}C	93
5.46	EDX analysis of 1 wt.% Pr: (a) 600 ^{o}C, (b) 700 ^{o}C, (c) 800 ^{o}C, (d) 900 ^{o}C, and (e) 1000 ^{o}C	96
5.47	EDX analysis of 2 wt.% Pr: (a) 600 ^{o}C, (b) 700 ^{o}C, (c) 800 ^{o}C, (d) 900 ^{o}C, and (e) 1000 ^{o}C	98
5.48	EDX analysis of 3 wt.% Pr: (a) 600 ^{o}C, (b) 700 ^{o}C, (c) 800 ^{o}C, (d) 900 ^{o}C, and (e) 1000 ^{o}C	101
5.49	EDX analysis of 4 wt.% Pr: (a) 600 ^{o}C, (b) 700 ^{o}C, (c) 800 ^{o}C, (d) 900 ^{o}C, and (e) 1000 ^{o}C	103
5.50	EDX analysis of 5 wt.% Pr: (a) 600 ^{o}C, (b) 700 ^{o}C, (c) 800 ^{o}C, (d) 900 ^{o}C, and (e) 1000 ^{o}C	106
5.51	UV-Vis absorption spectra of Pr addition in SLS-ZnO glass	107
5.52	UV-Vis absorption spectra of 0 wt.% Pr at 600, 700, 800, 900 and 1000 ^{o}C	108
5.53	UV-Vis absorption spectra of 1 wt.% Pr at 600, 700,	109

© COPYRIGHT UPM

	800, 900 and 1000 °C	
5.54	UV-Vis absorption spectra of 2 wt.% Pr at 600, 700, 800, 900 and 1000 °C	109
5.55	UV-Vis absorption spectra of 3 wt.% Pr at 600, 700, 800, 900 and 1000 °C	110
5.56	UV-Vis absorption spectra of 4 wt.% Pr at 600, 700, 800, 900 and 1000 °C	110
5.57	UV-Vis absorption spectra of 5 wt.% Pr at 600, 700, 800, 900 and 1000 °C	111
5.58	UV-Vis absorption spectra of various Pr concentration at 600 °C	112
5.59	UV-Vis absorption spectra of various Pr concentration at 700 °C	113
5.60	UV-Vis absorption spectra of various Pr concentration at 800 °C	113
5.61	UV-Vis absorption spectra of various Pr concentration at 900 °C	114
5.62	UV-Vis absorption spectra of various Pr concentration at 1000 °C	114
5.63	Plot of extinction coefficient (k) vs. hv of Pr addition in SLS-ZnO glass	116
5.64	Plot of $(\alpha hv)^{2/3}$ vs. hv of Pr addition in SLS-ZnO glass	116
5.65	Variation of optical band gap of Pr addition in SLS-ZnO glass	118
5.66	Plot of extinction coefficient (k) vs. hv of 0 wt.% Pr at 600, 700, 800, 900 and 1000 °C	119
5.67	Plot of $(\alpha hv)^{2/3}$ vs. hv for 0 wt.% Pr at 600, 700, 800, 900 and 1000 °C	119
5.68	Variation of the optical band gap of 0 wt.% Pr at 600, 700, 800, 900 and 1000 °C	121
5.69	Plot of extinction coefficient (k) vs. hv for 1 wt.% Pr at 600, 700, 800, 900 and 1000 °C	122

© COPYRIGHT UPM

5.70	Plot of extinction coefficient (k) vs. hv for 2 wt.% Pr at 600, 700, 800, 900 and 1000 ^{o}C	122
5.71	Plot of extinction coefficient (k) vs. hv for 3 wt.% Pr at 600, 700, 800, 900 and 1000 ^{o}C	123
5.72	Plot of extinction coefficient (k) vs. hv for 4 wt.% Pr at 600, 700, 800, 900 and 1000 ^{o}C	123
5.73	Plot of extinction coefficient (k) vs. hv for 5 wt.% Pr at 600, 700, 800, 900 and 1000 ^{o}C	124
5.74	Plot of $(\alpha hv)^{2/3}$ vs. hv for 1 wt.% Pr at 600, 700, 800, 900 and 1000 ^{o}C	124
5.75	Plot of $(\alpha hv)^{2/3}$ vs. hv for 2 wt.% Pr at 600, 700, 800, 900 and 1000 ^{o}C	125
5.76	Plot of $(\alpha hv)^{2/3}$ vs. hv for 3 wt.% Pr at 600, 700, 800, 900 and 1000 ^{o}C	125
5.77	Plot of $(\alpha hv)^{2/3}$ vs. hv for 4 wt.% Pr at 600, 700, 800, 900 and 1000 ^{o}C	126
5.78	Plot of $(\alpha hv)^{2/3}$ vs. hv for 5 wt.% Pr at 600, 700, 800, 900 and 1000 ^{o}C	126
5.79	Variation of optical band gap of 1 wt.% Pr at 600, 700, 800, 900 and 1000 ^{o}C	129
5.80	Variation of optical band gap of 2 wt.% Pr at 600, 700, 800, 900 and 1000 ^{o}C	129
5.81	Variation of optical band gap of 3 wt.% Pr at 600, 700, 800, 900 and 1000 ^{o}C	130
5.82	Variation of optical band gap of 4 wt.% Pr at 600, 700, 800, 900 and 1000 ^{o}C	130
5.83	Variation of optical band gap of 5 wt.% Pr at 600, 700, 800, 900 and 1000 ^{o}C	131
5.84	Variation of optical band gap of various Pr concentration at 600 ^{o}C	132
5.85	Variation of optical band gap of various Pr concentration at 700 ^{o}C	133
5.86	Variation of optical band gap of various Pr concentration at 800 ^{o}C	134

© COPYRIGHT UPM

5.87	Variation of optical band gap of various Pr concentration at 900 ^{o}C	135
5.88	Variation of optical band gap of various Pr concentration at 1000 ^{o}C	136
5.89	Emission spectrum of Pr addition in SLS-ZnO glass under excitation at 444 nm	137
5.90	Emission spectrum of 0 wt.% Pr at 600, 700, 800, 900 and 1000 ^{o}C	139
5.91	Emission spectrum of 1 wt.% Pr at 600, 700, 800, 900 and 1000 ^{o}C	139
5.92	Emission spectrum of 2 wt.% Pr at 600, 700, 800, 900 and 1000 ^{o}C	140
5.93	Emission spectrum of 3 wt.% Pr at 600, 700, 800, 900 and 1000 ^{o}C	140
5.94	Emission spectrum of 4 wt.% Pr at 600, 700, 800, 900 and 1000 ^{o}C	141
5.95	Emission spectrum of 5 wt.% Pr at 600, 700, 800, 900 and 1000 ^{o}C	141
5.96	Emission spectrum of various Pr concentration at 600 ^{o}C	143
5.97	Emission spectrum of various Pr concentration at 700 ^{o}C	143
5.98	Emission spectrum of various Pr concentration at 800 ^{o}C	144
5.99	Emission spectrum of various Pr concentration at 900 ^{o}C	144
5.100	Emission spectrum of various Pr concentration at 1000 ^{o}C	145
5.101	The energy level of Pr addition into SLS-ZnO glass ceramics	146

© COPYRIGHT UPM

LIST OF ABBREVIATIONS AND SYMBOLS

Zn_2SiO_4	Willemite
ZnO	Zinc Oxide
SiO_2	Silica Oxide
SLS	Soda Lime Silica
α	Alpha
β	Beta/ Constant
ϒ	Gama
Pr_6O_{11}	Praseodymium Oxide
WLEDs	White Light Emitting Diodes
LED	Light Emitting Diodes
Pr^{3+}	Trivalent Praseodymium
Wt.	Weight
T_g	Glass transition
T_c	Temperature Crystallization
XRD	X-ray Diffraction
DSC	Differential Scanning Calorimetry
FTIR	Fourier Transform Infrared Radiation
FESEM	Field Emission Scanning Microscopy
UV-Vis	Ultraviolet-Visible spectrometers
EDX or EDS	Energy Dispersive X-ray Spectroscopy
PL	Photoluminescence
E_u	Urbach energy
h	Plank constant
v	Phonon frequency
$\alpha(v)$	Absorption coefficient
hν	Photon energy
λ	Wavelength
k	Extinction coefficient.
E_g	Optical band gap

© COPYRIGHT UPM

CHAPTER 1

INTRODUCTION

1.1 Background of study

In recent years, special attention has been paid to the development of willemite (Zn_2SiO_4) for optical applications because of its unique properties, wide band gap (5.5 ev) and excellent chemical stability. Willemite was first discovered in 1829 in a "calamine" orebody in Belgium by Armand Le´vy in Moresne (Simonov et al., 1977). According to Takesue et al. (2009), the name of willemite was dedicated to King Willem of the Netherlands. Since then, the existence of willemite was found to be distributed all over the world.

Furthermore, Zn_2SiO_4 which formed the binary ZnO-SiO_2 phase system have also been employed extensively as host matrices of rare earth ions for applications in the area of luminescent materials. Hence, the increasing demand in this field has motivated researchers to develop novel inorganic Zn_2SiO_4 phosphor which used a low energy process that would help to solve both energy and environmental problems of our society. There are various methods to synthesize Zn_2SiO_4 such as solid state, sol-gel, hydohermal, solvothermal, co-precipitation, and spray pyrolysis method (Yang et al., 2013). Conventional solid- state method is important for fabrication of willemite due to its long history of practical use. This method involves the sintering and crystallisation of glass samples. Takesue et al. (2009) reported that the raw materials are well mixed and sintered at temperatures between 900 and 1500 ^oC for several hours in an electric furnace to form Zn_2SiO_4 inorganic phosphor. In brief, this method employed here involved the solid diffusion of atoms or atomic groups among solid raw materials. Solid-state methods provide irregularly shaped particles giving particle diameters of the order of microns with a wide size distribution. It was reported by Tammann and Kalsing (1925) that ZnO and SiO_2 react at around 775 ^oC to form Zn_2SiO_4 that is confirmed by the appearance of an exothermic peak with differential scanning calorimetry. The phases of Zn_2SiO_4 are produced by solid-diffusion of ZnO from the surface of SiO_2 are illustrated by the following equation (Leverenz and Urbach, 1950)

$$SiO_2 + 2ZnO = Zn_2SiO_4 \qquad (2.1)$$

Synthesis of Zn_2SiO_4 by sol- gel have had the lowest processing temperatures of all growth methods and produce spherical particles. Usually, this method involved a solvent, such as water, alcohol, ionic liquid and their mixtures at temperatures lower than the boiling point and at ambient pressure. Various Zn and dopant sources (e.g. nitrate, sulfate, chloride, acetate) and Si sources (e.g. silica, silicates, alkoxysilanes, water glass) are used as the starting materials. These materials are dissolved or dispersed in solvents and then mixed to produce a homogenous solution or uniform dispersion. The solutions or dispersions obtained are coated onto a substrate or simply dried. The phase formation of Zn_2SiO_4 by sol gel needs calcinations higher than 800

© COPYRIGHT UPM

^{o}C to form α-phase Zn_2SiO_4 (Takesue et al., 2009). Similarly of solid-state method, the sol gel method also involves in high temperatures and based on the diffusion in the solid state in order to produce α-phase Zn_2SiO_4.

The other methods such as hydrothermal and solvothermal can produce α-phase Zn_2SiO_4 without post calcinations. It is indicated that, the crystallization of α-phase Zn_2SiO_4 in solvent occurs at lower temperature than those required in solid diffusion. Generally, hydrothermal methods use water or an aqueous mixture as the reaction medium, while solvothermal methods use organic solvents. The method of hydrothermal and solvothermal are carried out in a Teflon-lined autoclave in which raw materials are loaded and then sintered at temperatures of 100 to 370 ^{o}C. However, this method produced a low crystallinity of Zn_2SiO_4 that have lower luminescence properties compared to the solid-state method.

In this study, the techniques of melt-quenching and solid state were used to produce Zn_2SiO_4 since it has many advantages such as simple process and large-scale production in the industrial operation than the chemical method. Soda Lime Silica (SLS) has been the focus of numerous investigations because of its potential for low temperature viscous flow sintering and promising as low cost integrated optical amplifier. Host matrix based on ZnO has attracted increasing interest because of its wide band gap and large exciting binding energy (60 mev) for application in optoelectronic devices. According to Qian et al. (2008), ZnO act as a network former that is connected to the neighboring SiO_4 to produce Si-O-Zn bond by bridging oxygen. Therefore, the combination of both SLS-ZnO is a promising host matrix for production of Zn_2SiO_4 phosphors due to their low melting point, good stability for rare earth ions and excellent properties in chemical stability and luminescence.

1.2 Phase formation of willemite

Recently, willemite ceramics were widely studied as luminescent material for their high stability and high efficiency. Therefore, the study of crystalline phases of Zn_2SiO_4 ceramics is very important in order to develop useful glass ceramics in optical field.

As shown in Figure 1.1, the melting temperature of Zn_2SiO_4 was 1498 ^{o}C instead of 1512°C as reported by Williamson and Glasser (1964). It forms a eutectic with tridymite at 1,432° C and 49.1 per cent ZnO. Eutectic with ZnO occurred at 1,507° C. and 77.5 mol per cent ZnO. According to the ZnO-SiO_2 binary phase diagram , α phase Zn_2SiO_4 was found in the 51.6 mol per cent ZnO, quenched at 1,440° C, and 65.0 mol per cent ZnO, quenched at 1,505° C. It is known, α phase Zn_2SiO_4 is the stable compound that can be synthesized at temperature greater than approximately 800 ^{o}C and at pressure greater than approximately 3 GPa (Syono et al., 1971). However, there are two metastable phase β-Zn_2SiO_4 and ϒ- Zn_2SiO_4 were reported in Williamson's study. β -Zn_2SiO_4 occurs in rapid cooling of liquid melt with composition between 33.3 and 63 mol% SiO_2, while ϒ- Zn_2SiO_4 is produced by rapid quenching in the compositional range of 45 to 55 mol% SiO_2.

© COPYRIGHT UPM

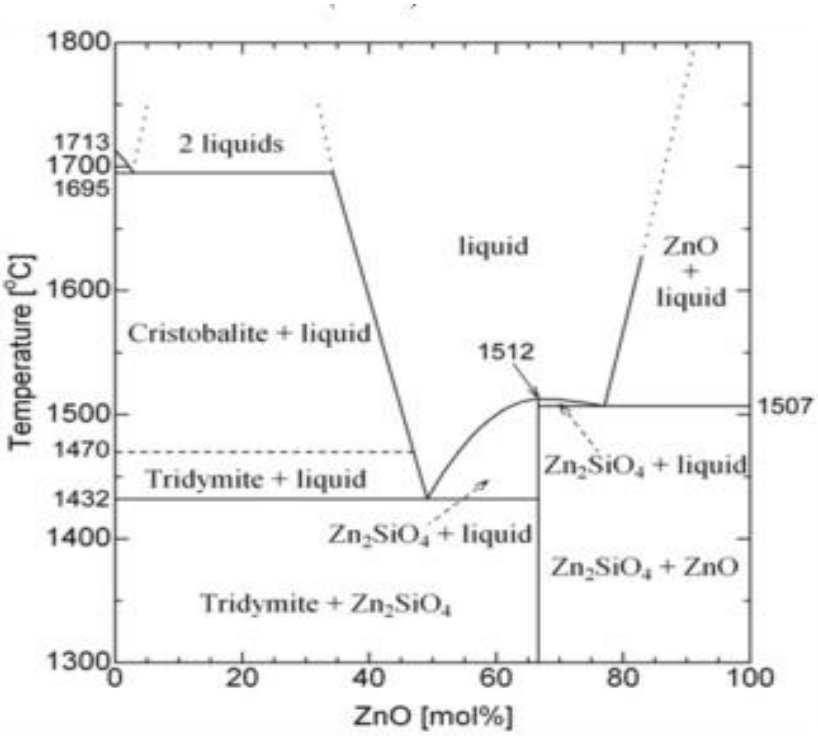

Figure 1.1: Equilibrium phase diagram for ZnO-SiO_2 system (Bunting, 1930)

Figure 1.2 shows α phase Zn_2SiO_4 is a neosilicate or orthosilicates that consist of isolated SiO_4^{4-} tetrahedrons and ZnO_4^{6-} in the zinc silica system. It was reported by Taylor (1962), that ZnO and SiO_2 react at around 775° C to form β-Zn_2SiO_4 which is confirmed by the appearance of an exothermic peak with differential scanning calorimetry. The transformation of orthorhombic - β phase into α -phase appeared at 835°C as an exothermic reaction according to thermal analysis methods Gotz and Masson (1978)

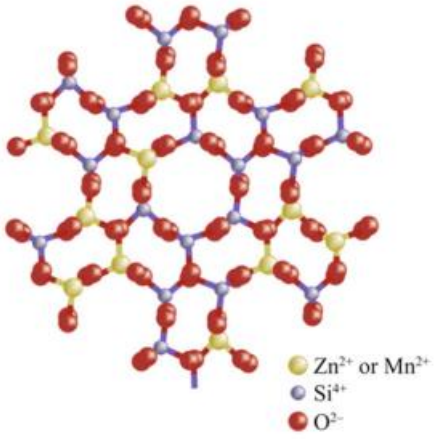

Figure 1.2: Crystalline structure of α phase Zn_2SiO_4 (Lukic et al., 2008)

© COPYRIGHT UPM

1.3 Significant and motivation of research

White Light Emitting Diodes (WLEDs) are of interest in optoelectronics field because of their benefits in terms of long lifetime, long energy consumption, high luminous efficiency and reliability. Generally, the most common technique to produce WLEDs by coating yellow phosphor on the surface GaN blue LED chips. However, they have low color rendering index due to lack of red content. Among rare earth materials, trivalent Praseodymium (Pr^{3+}) ions are considered as a promising red activator in host materials via red emission wavelengths at ~618 nm and ~650nm. Besides Pr^{3+} ions having strong blue excitation in the wavelength at ~450 nm. It is significant to search for a stable red phosphor with environmental friendliness under blue excitation for WLEDs application. Thus, this study has been focused on structural, luminescence and optical properties of Pr doped SLS-ZnO glass ceramics at varying sintering temperature for the production of low cost red Zn_2SiO_4 phosphors.

1.4 Problem statements

Nowadays, the combination of SiO_2-ZnO are of great interest as a host lattice for the fabrication of efficient optical system. However, pure SiO_2 glasses with high viscosity requires melting temperature at above 2000 ^oC may lead to high cost for mass production. Thus, SLS glasses are potential candidates for synthesizing SiO_2 would be an effective effort in reducing disposal cost and preserving environment. According to Chimalawong et al. (2010), SiO_2 glass is a suitable host matrix for rare earth ions due to its interesting properties such as good durability, good chemical stability and high UV transparency.

The production of Zn_2SiO_4 glass ceramics by utilizing SLS-ZnO glass may lead to high homogeneity, well controlled dopant concentration, easy fabrication and improved optical properties. From previous literatures (Gao, 2013), rare earth ions incorporated into glass ceramics enhanced PL properties by changing of ligand field around rare earth ions. Regarding to the enhancement of PL properties, Pr^{3+} is a very interesting rare earth ion which offers the possibility of simultaneous emission wavelength in the blue, green, orange, red and infrared region. However, there is limited report on Pr doped Zn_2SiO_4 glass ceramics system for optical and PL properties. Therefore, the knowledge of structural, thermal, optical and luminescence properties is a very useful tool in order to develop a new kind of Pr doped Zn_2SiO_4 glass ceramics for optoelectronic application.

© COPYRIGHT UPM

1.5 Objectives

1.5.1 Main research project objective

The main objective of this research project is to produce a low cost red emitting phosphor glass ceramic with strong absorption in the blue wavelength region. Generally, phosphor host material is based on Zn_2SiO_4 can be identified as a proper host material which achieves excellent luminescence. Trivalent Praseodymium (Pr^{3+}) ions doped into Zn_2SiO_4 matrix are interesting due to search for new material in the field of optoelectronic devices. Therefore, it is necessary to develop a red Zn_2SiO_4 phosphor based on SLS– ZnO host matrix doped with Pr without incorporating expensive materials.

1.5.2 Work-phase objectives

Hence, this research embarks on the following work-phase objectives which are:

1. To synthesize Zn_2SiO_4 based glass ceramics added with Pr_6O_{11} by conventional melt-quenching method.
2. To investigate the effect of Pr addition on structural, optical and luminescence properties of Zn_2SiO_4 at different sintering temperatures.
3. To study the effect of Pr^{3+} addition in Zn_2SiO_4 on phase formation and microstructure at different sintering temperatures.

1.6 Hypothesis

According to work phase objectives, this study is hypothesized as follows;

1. The glass transition would increase with increase of Pr content due to the formation of non-bridging oxygen in SLS-ZnO glass matrix, thus increasing the optical and luminescence properties.
2. The crystalline peaks of Pr addition in Zn_2SiO_4 would increase with increase in sintering temperature. It is expected that, Pr^{3+} would incorporate into the Zn_2SiO_4 host matrix in a successful substitution of Zn^{2+} by Pr^{3+} in the Zn_2SiO_4 framework.
3. Optical and luminescence properties of Pr addition in Zn_2SiO_4 would enhance with increase in sintering temperature. The introduction of Pr into Zn_2SiO_4 would achieve red emission intensity for the red phosphor.

© COPYRIGHT UPM

1.7 Thesis outline

The thesis is organised according to the following chapters. The general introduction of willemite, its phase formation and a statement of the motivation, problems as well as objectives and hypothesis of the research are provided in Chapter 1. In Chapter 2, the framework of research area is presented by literature surveys on density, thermal, structural, optical and luminescence properties of willemite materials. Chapter 3 describes the related theories on optical absorption and luminescence of glass and glass ceramics systems. The details of the experimental techniques employed in this research are discussed in Chapter 4. The results of the Pr addition willemite glass ceramics materials at different sintering temperatures are presented in Chapter 5. Chapter 6 summarizes the results as conclusion and suggestions for future work in Pr addition willemite system.

© COPYRIGHT UPM

REFERENCES

Abdel-Baki, M., Abdel-Wahab, F. A., Radi, A., & El-Diasty, F. (2007). Factors affecting optical dispersion in borate glass systems. *Journal of Physics and Chemistry of Solids*, *68*(8), 1457–1470

Al-Harbi, O. A. (2009). Effect of different nucleation catalysts on the crystallization of. *Ceramics International*, *35*, 1121–1128.

Alekseeva, I., Dymshits, O., Tsenter, M., Zhilin, A., Golubkov, V., Denisov, I., Yumashev, K. (2010). Optical applications of glass-ceramics. *Journal of Non-Crystalline Solids*, *356*(52–54), 3042–3058.

An, Y., Labbé, C., Khomenkova, L., Morales, M., Portier, X., & Gourbilleau, F. (2013). Microstructure and optical properties of Pr^{3+} -doped hafnium silicate films. *Nanoscale Research Letters*, *8*, 1–7.

Anjaiah, J., Laxmikanth, C., Veeraiah, N., & Kistaiah, P. (2015). Luminescence properties of Pr^{3+} doped $Li_2O - MO - B_2O_3$ glasses. *Journal of Luminescence*, *161*, 147–153

Annapurna, K., Chakrabarti, R., Buddhhudu, S. (2007). Absorption and emission spectral analysis of Pr 3 + : tellurite glasses. *Journal of Material Science*, *42*, 6755–6761.

Babu, B. C., & Buddhudu, S. (2013). Dielectric Properties of Willemite Zn_2SiO_4 Nano Powders by Sol-gel Method. *Physics Procedia*, *49*, 128–136.

Babu, K. S., Reddy, A. R., Reddy, K. V., & Mallika, A.N. (2014). High thermal annealing effect on structural and optical properties of ZnO-SiO_2 nanocomposite. *Materials Science in Semiconductor Processing*, *27*(1), 643–648.

Balaji, D., Durairajan, A., Thangaraju, D., Rasu, K. K., & Babu, S. M. (2013). Investigation of structural and luminescent properties of Pr^{3+} activated CsGd (WO_4) 2 by sol – gel synthesis. *Materials Science & Engineering B*, *178*(10), 762–767.

Basavaraj, R. B., Nagabhushana, H., Prasad, B. D., Sharma, S. C., Prashantha, S. C., & Nagabhushana, B. M. (2015). A single host white light emitting Zn_2SiO_4: Re $^{3+}$(Eu, Dy, Sm) phosphor for LED applications. *Optik-International Journal for Light and Electron Optics*,*126*(19), 1745-1756.

Bensalem, S., Chegaar, M., & Herguth, A. (2017). Band gap dependence with temperature of semiconductors from solar cells electrical parameters. *Current Applied Physics*, *17*, 55–59.

Berggren, K. F., & Sernelius, B. E. (1981). Band-gap narrowing in heavily doped many-valley semiconductors. *Physical Review B*, *24*(4), 1971-1986.

© COPYRIGHT UPM

Bernardo, E., Scarinci, G., Bertuzzi, P., Ercole, P., & Ramon, L. (2010). Recycling of waste glasses into partially crystallized glass foams. *Journal of Porous Material*, *17*, 359–365.

Berneschi, S., Bettinelli, M., Brenci, M., Conti, G. N., Pelli, S., Sebastiani, S., Righini, G. C. (2005). Aluminum co-doping of soda-lime silicate glasses: Effect on optical and spectroscopic properties. *Journal of Non-Crystalline Solids*, *351*(21–23), 1747–1753

Bonamartini C., A., Bondioli, F., Cannillo, V., Maria, F. A., Lancellotti, I., & Montorsi, M. (2005). The anorthite–diopside system: structural and devitrification study. Part I: structural characterization by molecular dynamic simulations. *Journal of the American Ceramic Society*, *88*(3), 714-718.

Bose, S., & Debnath, R. (2016). Optical characterization of Tm^{3+} in a high barium-tellurite glass in absence and presence of Yb^{3+} : Evidence of strong crystal-field effect and ef fi cient Yb^{3+}-Tm^{3+} energy transfer. *Journal of Luminescence*, *169*, 782–787.

Boutinaud, P., Mahiou, R., Cavalli, E., & Bettinelli, M. (2007). Red luminescence induced by intervalence charge transfer in Pr^{3+} - doped compounds. *Journal of Luminescence*, *123*, 430–433

Birkholz, M. (2006). *Thin film analysis by X-ray scattering*. John Wiley & Sons.

Bunting, E. N. (1930). Phase equilibria in the system SiO_2–ZnO. J*ournal of the American Ceramic Society*, *13*(1), 5-10.

Burtan-Gwizdala, B., Reben, M., Ryba-romanowski, W., Jarzabek, B., Mazurak, Z., Nosidlak, N., & Grelowska, I. (2015). The influence of Pr^{3+} content on luminescence and optical behavior of. *Optical Materials*, *47*, 231–236.

Cabral, A. C., Cavalcante, L. S., Deus, R. C., Longo, E., Simões, A. Z., & Moura, F. (2014). Photoluminescence properties of praseodymium doped cerium oxide nanocrystals. *Ceramics International*, *40*(3), 4445–4453

Calata, J. N. (2005). *Densification behavior of ceramic and crystallizable glass materials constrained on a rigid substrate* (Doctoral dissertation).

Carter, C. B., & Norton, M. G. (2007). *Ceramic materials: science and engineering*. Springer Science & Business Media.

Chen, D. D., Liu, Y. H., Zhang, Q. Y., Deng, Z. D., & Jiang, Z. H. (2005). Thermal stability and spectroscopic properties of Er^{3+}-doped niobium tellurite glasses for broadband amplifiers. *Materials Chemistry and Physics*, *90*(1), 78-82.

Chimalawong, P., Kaewkhao, J., Kedkaew, C., & Limsuwan, P. (2010). Optical and electronic polarizability investigation of Nd^{3+} -doped soda-lime silicate glasses. *Journal of Physical and Chemistry of Solids*, *71*(7), 965–970.

Condrate S. R. A. (1994). Infrared and raman spectra of glasses containing rare earth ions. In *Key Engineering Materials* (Vol. 94, pp. 209-232). Trans Tech Publications.

Cormier, L., Calas, G., & Beuneu, B. (2011). Structural changes between soda-lime silicate glass and melt. *Journal of Non-Crystalline Solids*, *357*(3), 926–931.

Davis, E. A., & Mott, N. (1970). Conduction in non-crystalline systems V. Conductivity, optical absorption and photoconductivity in amorphous semiconductors. *Philosophical Magazine*, *22*(179), 0903-0922

Diallo, P. T., Jeanlouis, K., Boutinaud, P., Mahiou, R., & Cousseins, J. C. (2001). Improvement of the optical performances of Pr^{3+} in $CaTiO_3$. *Journal of Alloys and Compounds*, *324*, 218–222.

Dolgonos, A., Mason, T. O., & Poeppelmeier, K. R. (2016). Direct optical band gap measurement in polycrystalline semiconductors: A critical look at the Tauc method. *Journal of Solid State Chemistry*, *240*, 43–48.

Dong, M., Yue, Z., Zhuang, H., Meng, S., & Li, L. (2008). Microstructure and Microwave Dielectric Properties of TiO_2 -Doped Zn_2SiO_4 Ceramics Synthesized Through the Sol–Gel Process. *Journal of the American Ceramic Society*, *3985*, 3981–3985

Du, M., Li, Y., Yuan, Y., Zhang, S., & Tang, B. (2007). A novel approach to $BaTiO_3$-based X8R ceramics by calcium borosilicate glass ceramic doping. *Journal of Electronic Materials*, *36*(10), 1389–1394.

Dwivedi, A., Joshi, C., & Rai, S. B. (2015). Effect of heat treatment on structural, thermal and optical properties of Eu^{3+} doped tellurite glass: formation of glass-ceramic and ceramics. *Optical Materials*, *45*, 202-208.

Ehrt, D. (2011). Photoactive glasses and glass ceramics. In *IOP Conference Series: Materials Science and Engineering* (Vol. 21, No. 1, p. 012001). IOP Publishing.

Elbatal, F. H., Azooz, M. A., & Hamdy, Y. M. (2009). Preparation and characterization of some multicomponent silicate glasses and their glass– ceramics derivatives for dental applications. *Ceramics International*, *35*, 1211–1218.

Egerton, R. F. (2007). *Physics Principles of Electron Microscopy: An Introduction to TEM, SEM, and AEM*. New York: Springer

El-Diasty, F., Abdel Wahab, F. A., & Abdel-Baki, M. (2006). Optical band gap studies on lithium aluminum silicate glasses doped with Cr^{3+} ions. *Journal of Applied Physics*,*100*(9), 093511.

El- Ghoul, J., Barthou, C., & El Mir, L. (2012). Synthesis, structural and optical properties of nanocrystalline vanadium doped zinc oxide aerogel. *Physica E:*

Low-Dimensional Systems and Nanostructures, *44*(9), 1910–1915.

El-Mallawany, R. (1999). Tellurite glasses Part 2 . Anelastic , phase separation , Debye temperature and thermal properties. *Materials Chemistry and Physics*, *60*, 103–131.

Elahi, M., Souri, D. (2006). Study of optical absorption and optical band gap determination of thin amorphous TeO_2 -V_2O_5 -MoO_3 blown films. *Indian Journal of Pure & Applied Physics*, *44*, 468–472.

Erol, M., Küçükbayrak, S., & Ersoy-Meriçboyu, A. (2008). Comparison of the properties of glass, glass-ceramic and ceramic materials produced from coal fly ash. *Journal of Hazardous Materials*, *153*(1–2), 418–425.

Esmaeili, A. (2016). Many-body , Pauli blocking and carrier-impurity interaction effects on the band gap of aluminum doped zinc oxide thin fi lms : A new method to evaluate both hole and electron effective masses of degenerate semiconductors. *Current Applied Physics*, *16*, 949–955

Faznny, M. F., Halimah, M. K., & Azlan, M. N. (2016). Effect of lanthanum oxide on optical properties of zinc borotellurite glass system. *Journal of Optoelectronics and Biomedical Materials*, *8*(2), 49–59.

Gaafar, M. S., & Marzouk, S. Y. (2007). Mechanical and structural studies on sodium borosilicate glasses doped with Er 2 O 3 using ultrasonic velocity and FTIR spectroscopy. *Physica B: Condensed Matter*, *388*(1), 294-302.

Gaˆcon, J. C., Horchani, K., Jouini, A., Dujardin, C., & Kamenskikh, I. (2006). Optical properties of praseodymium concentrated phosphates. *Optical Materials*, *28*, 14–20.

Gao, G. (2013). Tunable photoluminescence from rare earth and transition metal ions activated silicate glasses and glass ceramics Dissertation. In *University of Jena, China*.

Gilliot, P., Muller, D., Slaoui, A., Colis, S., & Dinia, A. (2014). Luminescent Properties and Energy Transfer in Pr^{3+} Doped and Pr^{3+} - Yb^{3+} Co-doped ZnO Thin Films. *The Journal of Physical Chemistry*, *118*, 13775–13780.

Gonçalves, M. C., Santos, L. F., & Almeida, R. M. (2002). Rare-earth-doped transparent glass ceramics. *Académie Des Sciences*, *5*, 845–854.

Götz, J., & Masson, C. R. (1978). Trimethylsilyl derivatives for the study of silicate structures. Part 4. The conversion of hemimorphite into willemite. *Journal of the Chemical Society, Dalton Transactions*, (9), 1134-1138.

Guo, H., Wang, Y., Gong, Y., Yin, H., Mo, Z., Tang, Y., & Chi, L. (2016). Optical band gap and photoluminescence in heavily Tb^{3+} doped GeO_2-B_2O_3-SiO_2-Ga_2O_3 magneto-optical glasses. *Journal of Alloys and Compounds*, *686*, 635–640.

© COPYRIGHT UPM

Gutzow, I., & Shmelzer, J. (1995). The Vitreous State-Structure, Thermodynamics, Rheology and Crystallisation. *Berlin, New York*.

Hamberg, I., & Granqvist, C. G. (1984). Band-gap widening in heavily Sn-daped In_2O_3. *Physical Review B*, *30*(6), 3240–3248.

Hamnabard, Z., Khalkhali, Z., Sadat, S., Qazvini, A., & Baghshahi, S. (2012). Preparation , heat treatment and photoluminescence properties of V-doped ZnO-SiO_2-B_2O_3 glasses. *Journal of Luminescence*, *132*(5), 1126–1132.

Harani, R., Hogarth, C. A., Ahmed, M. M., & Morris, D. F. C. (1984). Optical absorption spectra of praseodymium phosphate glasses. *Journal of Materials Science Letter*, *3*, 843–844.

Harris, D.C., *Quantitative Chemical Analysis*. 7th Edition, W.H. Freeman and Company, New York. 2006

Hasegawa, S., & Kitagawa, M. (1978). Effects of annealing on localized states in amorphous Ge films. *Solid State Communications*, *27*(9), 855-858.

Heath, J. and Taylor, N. *Energy Dispersive Spectroscopy*. 2nd ed., John Wiley & Sons,: Chichester. 2015

https://www2.chemistry.msu.edu/faculty/reusch/virttxtjml/spectrpy/uv-vis/uvspec.htm

http://www.psrc.usm.edu/macrog/dsc.htm

Hu, A. M., Li, M., Dali, D. L. M., & Liang, K. M. (2005). Crystallization and properties of a spodumene-willemite glass ceramic. *Thermochimica Acta*, *437*, 110–113.

Ilanchezhiyan, P., Kumar, G. M., Subramanian, M., & Jayavel, R. (2010). Effect of Pr doping on the structural and optical properties of ZnO nanorods. *Materials Science and Engineering: B*, *175*(3), 238–242

Inoue, Y., Okamoto, M., Kawahara, T., & Morimoto, J. (2006a). Photoacoustic spectra on Pr doped ZnO powders. *Journal of Alloys and Compounds*, *408*, 1234–1237.

Inoue, Y., Toyoda, T., Morimoto, J. (2006b). Evaluation of Co- and Pr-Doped Zinc Silicate Powders by Photoacoustic Spectroscopy. *Japanese Journal of Applied Physics*, *45*, 4601–4608.

Inoue, Y., Toyoda, T., & Morimoto, J. (2008). Photoacoustic spectra on Mn-doped zinc silicate powders by evacuated sealed silica tube method. *Journal of Material Science*, *43*, 378–383.

Irfanullah, M., & Iftikhar, K. (2011). The Correlation Between f – f Absorption and Sensitized Visible Light Emission of Luminescent Pr (III) Complexes : Role of Solvents and Ancillary Ligands on Sensitivity. *Journal of Fluorescence*,

© COPYRIGHT UPM

21, 673–686.

Jlassi, I., Elhouichet, H., & Ferid, M. (2016). In fl uence of MgO on structure and optical properties of alumino-lithium-phosphate glasses. *Physica E: Low-Dimensional Systems and Nanostructures*, *81*, 219–225.

Joshi, K., Rawat, M., Gautam, S. K., Singh, R. G., Ramola, R. C., & Singh, F. (2016). Band gap widening and narrowing in Cu-doped ZnO thin films. *Journal of Alloys and Compounds*, *680*, 252–258.

Jule, L. T., Dejene, F. B., Ali, A. G., Roro, K. T., Hegazy, A., Allam, N. K., & El, E. (2016). Wide visible emission and narrowing band gap in Cd-doped ZnO nanopowders synthesized via sol-gel route. *Journal of Alloys and Compounds*, *687*, 920–926.

Juoi, J. M., Arudra, D., Rosli, M., Hussain, K., & Japper, A. (2013). Microstructural properties of glass composite material made from incinerated scheduled waste slag and soda lime silicate (SLS) waste glass. *Journal of Non-Crystalline Solids*, *367*, 8–13.

Kaminskii, A. A., Zhavoronkov, N. I., & Mikhailov, V. P. (1993). A high-power praseodymium laser based on a rhombic crystal of $YAlO_3$-Pr^{3+}. In *Physics-Doklady*, *38*, 156-157.

Karamanov, A., & Pelino, M. (1999). Evaluation of the degree of crystallisation in glass-ceramics by density measurements. *Journal of the European Ceramic Society*, *19*(5), 649–654.

Karazhanov, S. Z., Ravindran, P., Fjellvg, H., & Svensson, B. G. (2009). Electronic structure and optical properties of ZnSiO3 and Zn2SiO4. *Journal of Applied Physics*, *106*(12), 1–7

Kashif, I., Soliman, A. A, Sakr, E. M., & Ratep, A. (2012). Effect of different conventional melt quenching technique on purity of lithium niobate ($LiNbO_3$) nano crystal phase formed in lithium borate glass. *Results in Physics*, *2*, 207–211.

Kaur, G., Kumar, M., Arora, A., Pandey, O. P., & Singh, K. (2011). Influence of Y_2O_3 on structural and optical properties of SiO_2– BaO– ZnO– xB_2O_3– ($10 - x$) Y_2O_3 glasses and glass ceramics. *Journal of Non-Crystalline Solids*, *357*, 858–863.

Kim, J. J., Bishop, S. R., Thompson, N., Kuru, Y., & Tuller, H. L. (2012). Optically derived energy band gap states of Pr in ceria. *Solid State Ionics*, *225*, 198–200

Kingery, W. D., Bowen, H. K., & Uhlmann, D. R. (1976). Grain growth, sintering and vitrification. *Introduction to Ceramics*, *2*, 448-515.

Krsmanovi, R. Ć., Anti, Ž. Ć., Marinovi, M. Ć. Ć., & Anin, M. D. D. Ć. (2009).

© COPYRIGHT UPM

Samarium and terbium doped Zn_2SiO_4 powders obtained by polymer induced sol-gel synthesis. *Journal of Optoelectronics and Advanced Materials-Symposia*, *1*(1), 37–41.

Kohale, R. L., & Dhoble, S. J. (2012). Luminescence in Eu^{2+}-activated microcrystalline pyrophosphor. *Micro & Nano Letters*, *7*(5), 453-455.

Lakshminarayana, G., Kaky, M. K., Baki, O. S., Ye, S., Lira, A., Kityk, V. I., & Mahdi, A. M. (2016). Concentration dependent structural , thermal, and optical features of Pr^{3+} -doped multicomponent tellurite glasses. *Journal of Alloys and Compounds*, *686*, 769–784.

Layek, A., De, S., Thorat, R., & Chowdhury, A. (2011). Spectrally resolve photoluminescence imaging of ZnO nanocrystals at single-particle levels. *The Journal of Physical Chemistry Letters*, *2*(11), 1241-1247.

Leverenz, H. W., & Urbach, F. (1950). Introduction to the Luminescence of Solids. *Physics Today*,*3*, 32.

Li, B. O., Yuan, Y., Zhang, S., & Jiang, H. (2011). Microstructure and microwave dielectric properties of $(Zn1 – x Mg x)_2 SiO_4$ ceramics. *Bulletin of Materials. Science*, *34*(4), 921–925.

Li, G., Long, T., Song, Y., Gao, G., Jijing, X.U., Baichao, A.N., Shucai, G.A.N., Hong, G. (2010a). Preparation and luminescent properties of $CaAl_2O_4:Eu_{3+},R^+$ (R=Li, Na, K) phosphors. *Journal of Rare Earths*, *28*(1), 22–25.

Li, H., Lu, G., Wang, Y., Guo, Y., & Guo, Y. (2010b). Synthesis of flower-like La or Pr-doped mesoporous ceria microspheres and their catalytic activities for methane combustion. *Catalysis Communications*, *11*(11), 946-950.

Li, H., Luo, K., Xia, M., & Wang, P. W. (2014). Synthesis and optical properties of Pr^{3+}-doped ZnO quantum dots. *Journal of Non-Crystalline Solids*, *383*, 176–180.

Li, Y. C., Chang, Y. H., Lin, Y. F., Chang, Y. S., & Lin, Y. J. (2007). Luminescent properties of trivalent praseodymium-doped lanthanum aluminum germanate $LaAlGe_2O_7$. *Journal of Physics and Chemistry of Solids*, *68*(10), 1940–1945.

Lim, S. G., Kriventsov, S., Jackson, T. N., Haeni, J. H., Schlom, D. G., Balbashov, A. M., Uecker, R., Freeouf, J. L., Lucovsky, G. (2002). Dielectric functions and optical bandgaps of high- K dielectrics for metal-oxide-semiconductor field-effect transistors by far ultraviolet spectroscopic ellipsometry. *Journal of Applied Physics*, *91*(7), 4500–4505.

Lin, B., Fu, Z., & Jia, Y. (2001). Green luminescent center in undoped zinc oxide films deposited on silicon substrates. *Applied Physics Letters*, *79*(7), 943–945.

Lin, C. M., Tsai, Y. Z., & Chen, J. S. (2007). The microstructure and cathodoluminescence characteristics of sputtered Zn_2SiO_4 : Ti phosphor thin

films. *Thin Solid Films*, *515*, 7994–7999.

Lin, J. ., Sanger, U. D., Mennig, M., & Barner, K. (2000). Sol ± gel deposition and characterization of Mn 2 1 -doped silicate phosphor films. *Thin Solid Films*, *360*, 39–45.

Loh, Z. H., Samanta, A. K., & Sia Heng, P. W. (2014). Overview of milling techniques for improving the solubility of poorly water-soluble drugs. *Asian Journal of Pharmaceutical Sciences*, *10*(4), 255–274

Lu, J. G., Fujita, S., Kawaharamura, T., Nishinaka, H., Kamada, Y., Ohshima, T., Ye, Z.Z., Zheng, J.Y., Zhang, Z.Y., Zhu, P.L., He, P.H., Zhao, H. B. (2007). Carrier concentration dependence of band gap shift in n -type ZnO : Al films. *Journal of Applied Physics*, *101*, 12–14.

Lu, Q., Wang, P., & Li, J. (2011). Structure and luminescence properties of Mn-doped Zn_2SiO_4 prepared with extracted mesoporous silica. *Materials Research Bulletin*, *46*(6), 791–795.

Lukic', S. R., Petrovic´, D. M., Drami'canin, M. D., Mitric', M., & Dacanin, L. (2008). Optical and structural properties of Zn_2SiO_4 : Mn 2+ green phosphor nanoparticles obtained by a polymer-assisted sol–gel method. *Scripta Materialia*, *58*, 655–658.

Mahamuda, S., Swapna, K., Rao, A. S., Sasikala, T., & Moorthy, L. R. (2013). Reddish-orange emission from Pr^{3+} doped zinc alumino bismuth borate glasses. *Physica B*, *428*, 36–42.

Marinoni, N., Alessio, D. D., Diella, V., Pavese, A., & Francescon, F. (2013). Effects of soda e lime e silica waste glass on mullite formation kinetics and micro-structures development in vitreous ceramics. *Journal of Environmental Management*, *124*, 100–107.

Masuno, A., Inoue, H., Yu, J., & Arai, Y. (2010). Refractive index dispersion, optical transmittance, and Raman scattering of $BaTi_2O_5$ glass. *Journal of Applied Physics*, *108*(63520), 1–5.

Matori, K. A., Zaid, M. H. M., Sidek, H. A. A., Halimah, M. K., Wahab, Z. A., & Sabri, M. G. M. (2010). Influence of ZnO on the ultrasonic velocity and elastic moduli of soda lime silicate glasses. *International Journal of Physical Sciences*, *5*(14), 2212-2216.

Matteucci, F., Dondi, M., & Guarini, G. (2002). Effect of soda-lime glass on sintering and technological properties of porcelain stoneware tiles. *Ceramics International*, *28*(8), 873-880.

Mitang, W., Cheng, J., & Mei, L. I. (2010). Effect of rare earths on viscosity and thermal expansion of soda-lime-silicate glass. *Journal of Rare Earths*, *28*, 308-311

© COPYRIGHT UPM

Mishra, K. C., Johnson, K. H., DeBoer, B. G., Berkowitz, J. K., Olsen, J., Dale, E. A. (1991). First principles investigation of electronic structure and associated properties of zinc orthosilicate phosphors. *Journal of Luminescence*, *47*(5), 197–206.

Mott, N. F., & Davis, E. A. (1971). *Electronic process in non-crystalline materials*. Oxford University Press.

Omar, N. A. S., Fen, Y. W., Matori, K. A., Zaid, M. H. M., & Samsudin, N. F. (2016). Structural and optical properties of Eu^{3+} activated low cost zinc soda lime silica glasses. *Results in Physics*, *6*, 640–644.

Omri, K., Ghoul, E. J., Alyamani, A., Barthou, C., & Mir, E. L. (2013). Luminescence properties of green emission of SiO_2 / Zn_2SiO_4 : Mn nanocomposite prepared by sol – gel method. *Physica E*, *53*, 48–54.

Pal, I., Agarwal, A., Sanghi, S., & Aggarwal, M. P. (2011). Structural, absorption and fluorescence spectral analysis of Pr^{3+} ions doped zinc bismuth borate glasses. *Journal of Alloys and Compounds*, *509*(28), 7625–7631.

Park, J., Park, K., Lee, S., Kim, J., Kim, G., & Yoo, J. (2013). A simple synthesis method for Zn_2SiO_4 : Mn^{2+} phosphor films and their optical and luminescence properties. *Journal of Luminescence*, *134*, 71–74.

Pawar, P. P., Munishwar, S. R., & Gedam, R. S. (2016). Physical and optical properties of Dy^{3+} / Pr^{3+} Co-doped lithium borate glasses for W-LED. *Journal of Alloys and Compounds*, *660*, 347–355.

Pfeiffer, H. G., & Fonda, G. R. (1952). The zinc silicate phosphors fluorescing in the yellow and red. *Journal of the Electrochemical Society*, *99*(4), 140-143.

Plaza, J. L., & Aragó, C. (2015). Characterisation of pure and Pr doped BiB_3O_6 glasses prepared under different thermal conditions. *Journal of Alloys and Compounds*, *623*, 178–185.

Prado, M. O., Fredericci, C., & Zanotto, E. D. (2003). Non-isothermal sintering with concurrent crystallization of polydispersed soda–lime–silica glass beads. *Journal of non-crystalline solids*, *331*(1), 157-167.

Qian, G., Baccaro, S., Falconieri, M., Bei, J., Cecilia, A., & Chen, G. (2008). Photoluminescent properties and Raman spectra of ZnO-based scintillating glasses. *Journal of Non-Crystalline Solids*, *354*(40–41), 4626–4629.

Rada, M., Culea, E., Rada, S., Bot, A., Aldea, N., & Rednic, V. (2012). Anomalies of some physical properties and electrochemical performance of lithium – lead – germanate glasses. *Journal of Non-Crystalline Solids*, *358*(23), 3129–3136.

Rahman, M. M., Khan, M. K. R., Islam, M. R., Halim, M. A., Shahjahan, M., Hakim, M. A.,Saha, D.K., Khan, J. U. (2012). Effect of Al Doping on Structural , Electrical , Optical and Photoluminescence Properties of Nano-Structural

© COPYRIGHT UPM

ZnO Thin Films. *Journal of Materials Science & Technology*, *28*(4), 329–335.

Rajagukguk, J., Kaewkhao, J., Djamal, M., Hidayat, R., & Ruangtaweep, Y. (2016). Structural and optical characteristics of Eu^{3+} ions in sodium-lead- zinc-lithium-borate glass system. *Journal of Molecular Structure*, *1121*, 180–187.

Ramos-Brito, F., Garcia-Hipolito, M., Alejo-Armenta, C., Alvarez-Fragoso, O., Falcony., C. (2007). Characterization of luminescent praseodymium-doped ZrO_2 coatings deposited by ultrasonic spray pyrolysis. *Journal of Physics D: Applied Physics*, *6718*(40), 6718–6724.

Ramos-Brito, F., García-Hipólito, M., Martínez-Martínez, R., Martínez-Sánchez, E., & Falcony, C. (2004). Preparation and characterization of photoluminescent praseodymium-doped ZrO_2 nanostructured powders. *Journal of Physics D: Applied Physics*, *37*(5), L13–L16.

Raimondo, M., Zanelli, C., Matteucci, F., Guarini, G., Dondi, M., & Labrincha, J. A. (2007). Effect of waste glass (TV/PC cathodic tube and screen) on technological properties and sintering behaviour of porcelain stoneware tiles. *Ceramics International*, *33*(4), 615-623.

Rada, M., Culea, E., Rada, S., Bot, A., Aldea, N., & Rednic, V. (2012). Anomalies of some physical properties and electrochemical performance of lithium – lead – germanate glasses. *Journal of Non-Crystalline Solids*, *358*(23), 3129–3136.

Ramteke, D. D., Annapurna, K., Deshpande, V. K., & Gedam, R. S. (2014). Effect of Nd^{3+} on spectroscopic properties of lithium borate glasses. *Journal of Rare Earths*, *32*(12), 1148-1153.

Ronda, C. R. (Ed.). (2007). *Luminescence: from theory to applications*. John Wiley & Sons

Rubem, O., Montedo, K., Hotza, D., Pedro, A., Oliveira, N. De, Meszaros, R.,Travitzky, N., Greil, P. (2012). Crystallisation Kinetics of a β - Spodumene-Based Glass Ceramic. *Advances in Materials Science and Engineering*, *2012*.

Sadat, S., Qazvini, A., Hamnabard, Z., Khalkhali, Z., & Baghshahi, S. (2012). Photoluminescence and microstructural properties of $SiO_2 – ZnO – B_2O_3$ system containing TiO_2 and V_2O_5. *Ceramics International*, *38*, 1663–1670.

Sangiorgi, N., Aversa, L., Tatti, R., Verucchi, R., & Sanson, A. (2017). Spectrophotometric method for optical band gap and electronic transitions determination of semiconductor materials. *Optical Materials*, *64*, 18–25.

Sawant, S.D., Baravkar, A.A., Kale, R.N. (2011). FTIR spectroscopy: principle, technique and mathematics. *International Journal of Pharma and Bio Sciences*. (2): 513-519.

© COPYRIGHT UPM

Sasikala, S., Pavithran, C., & Sebastian, T. M. (2010). Effect of lithium magnesium zinc borosilicate glass addition on densification temperature and dielectric properties of Mg 2SiO 4 ceramics. *Journal of Materials Science: Materials in Electronics*, *21*(2), 141–144.

Selomulya, R., Ski, S., Pita, K., Kam, C. ., Zhang, Q. ., & Buddhudu, S. (2003). Luminescence properties of $Zn_2SiO_4:Mn^{2+}$ thin-films by a sol–gel process. *Materials Science and Engineering: B*, *100*(2), 136–141.

Seitz., F. (1938). An interpretation of crystal luminescence. *Article Online*, *2*, 487–496.

Sharma, P., & Bhatti, H. S. (2009). Laser induced down conversion optical characterizations of synthesized Zn_2-x$MnxSiO_4$ ($0.5 \leq x \leq 5$ mol%) nanophosphors. *Journal of Alloys and Compounds*, *473*(1–2), 483–489.

Sharma, Y.K., Mathur, S.C., Dube, D. C. (1995). Optical absorption spectra and energy band gap in praseodymium borophosphate glasses. *Journal of Materials Science Letters*, *14*, 71–73.

Shasmal, N., & Karmakar, B. (2016). Enhancement and tuning of photoluminescence properties in Pr^{3+} / Au co-doped antimony oxide glass nanocomposites by thermal treatment. *Journal of Alloys and Compounds*, *688*, 313–322.

Shinde, K. N., Dhoble, S. J., Swart, H. C., & Park, K. (2012). Introduction. In *Phosphate Phosphors for Solid-State Lighting* (pp. 1-39). Springer Berlin Heidelberg.

Simonov, M. A., Sandomirskii, P. A., Tgorov-Tismenko, Y. K., & Belov, N. V. (1977, November). The crystal structure of willemite Zn_2SiO_4. In *Soviet Physics Doklady* (Vol. 22, p. 622).

Sindhu, S., Sanghi, S., Agarwal, A., Seth, V. P., & Kishore, N. (2005). Effect of Bi_2O_3 content on the optical band gap, density and electrical conductivity of $MO{\cdot}Bi_2O_3{\cdot}B_2O_3$ (M=Ba, Sr) glasses. *Materials Chemistry and Physics*, *90*(1), 83–89.

Slater, J. C., and Johnson, K. H. (1972). Self-consistent-field X α cluster method for polyatomic molecules and solids. *Physical Review B*, *5*(3), 844.

Souza, G. P., Rambaldi, E., Tucci, A., Esposito, L., & Lee, W. E. (2004). Microstructural Variation in Porcelain Stoneware as a Function of Flux System. *Journal of the American Society*, *1966*, 1959–1966.

Sreedharan, R. S., Vinodkumar, R., Navas, I., Prabhu, R., & Pillai, V. P. M. (2016). Influence of Pr Doping on the Structural , Morphological , Optical , Luminescent and Non-linear Optical Properties of RF-Sputtered ZnO Films. *The Minerals, Metals & Materials Society Influence*, *68*(1), 341–350.

Srivastava, A. M., & Duclos, S. J. (1997). On the luminescence of YF3-Pr^{3+} under vacuum ultraviolet and X-ray excitation. *Chemical physics letters*, *275*(5-6),

© COPYRIGHT UPM

453-456.

Stookey, S. D. (1961). *U.S. Patent No. 2,971,853*. Washington, DC: U.S. Patent and Trademark Office.

Sudhahar, S., Kumar, M. K., Jayaramakrishnan, V., Muralidharan, R., & Kumar, R. M. (2014). Effect of Sm+ Rare Earth Ion on the structural, thermal , mechanical and optical properties of potassium hydrogen phthalate single crystals. *Journal of Materials Science & Technology*, *30*(1), 13–18.

Suwanboon, S., Amornpitoksuk, P., & Bangrak, P. (2011). Synthesis, characterization and optical properties of Zn_1−xTixO nanoparticles prepared via a high-energy ball milling technique. *Ceramics International*, *37*(1), 333–340.

Suszynska, M., & Macalik, B. (2001). Optical studies in gamma-irradiated commercial soda–lime silicate glasses. *Nuclear Instruments and Methods in Physics Research Section B: Beam Interactions with Materials and Atoms*, *179*(3), 383-388.

Syono, Y., Akimoto, S. I., & Matsui, Y. (1971). High pressure transformations in zinc silicates. *Journal of Solid State Chemistry*, *3*(3), 369-380

Tandon, S.P., Surana, S.S.L., Tandon, K., Sule, K.K., Bhutra, M.P., Govil, R.C., Bishnoi N.B and Sharma Y.K., AR & DB Defence Project Report No 393 (1989).

Takesue, M., Hayashi, H., and Richard L.S.R. (2009). Thermal and chemical methods for producing zinc silicate (willemite): A review. *Progress in Crystal Growth and Characterization of Materials*, *55*(3–4), 98–124.

Talwatkar, S. S., Sunatkari, A. L., Tamgadge, Y. S., Pahurkar, V. G., & Muley, G. G. (2015). Influence of Li + and Nd 3+ co-doping on structural and optical properties of L -arginine-passivated ZnS nanoparticles. *Applied Physics A*, *118*, 675–682.

Tammann, G., and Kalsing, H. (1925). Chemical Reactions in Powdered Mixtures of Two Kinds of Crystals: IV, Behavior of V_2O_6, SiO_2, TiO_2, ZrO_2, Sb_2O_3, and As_2O_3 with Basic Oxides. *Z. anorg. u. allgem. Chem*, *149*, 68-69.

Tarafder, A., Molla, A. R., Dey, C., & Karmakar, B. (2013). Thermal, structural, and enhanced photoluminescence properties of Eu^{3+}-doped transparent willemite glass-ceramic nanocomposites. *Journal of the American Ceramic Society*, *96*(8), 2424–2431.

Tarafder, A., Rahaman, A., Mukhopadhyay, S., & Karmakar, B. (2014). Fabrication and enhanced photoluminescence properties of Sm^{3+} -doped ZnO – Al_2O_3 – B_2O_3 – SiO_2 glass derived willemite glass – ceramic nanocomposites. *Optical Materials*, *36*, 1463–1470.

Tauc, J. (1974). Optical properties of amorphous semiconductors. In *Amorphous and*

Liquid Semiconductors (pp. 159-220). Springer US.

Taylor, H. F. W. (1962). The dehydration of hemimorphite. *American Mineral*. 47, 932-944.

Tsai, M., Lu, Y., & Wang, Y. (2010). Synthesis and characterization of manganese-doped zinc orthosilicate phosphor powders. *Journal of Alloys and Compounds*, *505*(2), 818–823.

Tsai, M., Wu, J., Lu, Y., & Chang, H. (2011). Synthesis and luminescence characterization of manganese-activated willemite gel films. *Thin Solid Films*, *520*(3), 1027–1033.

Walsh, A., Silva, D. F. L. J., & Wei, H. S. (2008). Origins of band-gap renormalization in degenerately doped semiconductors. *Physical Review B*, *78*, 1–5.

Wang, D., Yin, Q., & Li, Y. (2002). Concentration quenching of Eu^{2+} in $SrO\ 6Al_2O_3 : Eu^{2+}$ phosphor. *Journal of Material Science*, *7*, 381–383.

Wang, M., Cheng, J., Li, M., & He, F. (2011). Structure and properties of soda lime silicate glass doped with rare earth. *Physica B: Physics of Condensed Matter*, *406*(2), 187–191.

Wang, M., Cheng, J., Li, M., He, F., & Deng, W. (2012). Viscosity and thermal expansion of soda-lime-silica glass doped with Gd_2O_3 and Y_2O_3. *Solid State Sciences*, *14*(8), 1233–1237.

Wang, T., Zhang, X., Wen, J., Chen, T., Ma, X., & Gao, H. (2014). Diameter-dependent luminescence properties of ZnO wires by mapping. *Journal of Physics D: Applied Physics*, *47*(17), 175304.

Wang, X., Zhuang, J., & Li, Y. (2004). Pr 6 O 11 Single-Crystal Nanotubes from a Molten-Salt Synthetic Method. *European Journal of Inorganic Chemistry*, 946–948.

Wen, W., Xuan, Y., Yin, J. N., & Xie, J. (2015). Influence of praseodymium doping concentration on the structural and optical properties of strontium molybdate crystals. *Res Chem Intermed*, *41*, 2479–2488.

Williamson, J., & Glasser, F. P. (1964). A new silica-like phase with simple cubic structure. *Nature*, *201*(4916), 286-287

Yamane, M., & Asahara, Y. (2000). *Glasses for photonics*. Cambridge University Press.

Yang, R., Xiaoye, H., Tao, L., Xinmu, Z., Xuezhen, Z., Yongxiu, L. (2011). Pr^{3+} - doped Li_2SrSiO_4 red phosphor for white LEDs. *Journal of Rare Earths*, *29*(3), 198–201.

Yang, R., Peng, Y., Lai, H., Chu, C., Chiou, B., & Su, Y. (2013). Effect of the different

© COPYRIGHT UPM

concentrations of Eu^{3+} ions on the microstructure and photoluminescent properties of Zn_2SiO_4 : x Eu^{3+} phosphors and synthesized with TEOS solution as silicate source. *Optical Materials*, *35*(9), 1719–1723.

Yang, X., Liu, J., Yang, H., Yu, X., Guo, Y., & Zhou, Y. (2009). Synthesis and characterization of new red phosphors for white LED applications. *Journal of Material Chemistry*, *19*, 3771.

Yu, Y., Zhu, X., Zhang, X., Yuan, J., Yu, H., Kuang, F., Xiong, Z., Liao, J., Zhang, W., Wang, G.,(2016). Growth and optical properties of Pr^{3+} : $KLu(WO_4)_2$ laser crystal : a candidate for red emission laser. *The Optical Society of Japan*, *23*, 391–400.

Zaid, M. H. ., Matori, K. ., Aziz, S. A., Kamari, H. M., Wahab, Z. A., Effendy, N., & Alibe, I. M. (2016). Comprehensive study on compositional dependence of optical band gap in zinc soda lime silica glass system for optoelectronic applications. *Journal of Non-Crystalline Solids*, *449*, 107–112.

Zaid, M. H. M., Matori, K. A., Aziz, S. A., Zakaria, A., & Ghazali, M. S. M. (2012). Effect of ZnO on the Physical Properties and Optical Band Gap of Soda Lime Silicate Glass. *International Journal of Molecular Sciences*, *13*, 7550–7558.

Zaman, F., Kaewkhao, J., Rooh, G., Srisittipokakun, N., & Kim, J. H. (2016). Optical and luminescence properties of Li_2O - Gd_2O_3 -MOB_2O_3 - Sm_2O_3 (($MOBi_2O_3$, BaO) glasses. *Journal of Alloys and Compounds*, *676*, 275–285.

Zamratul, M. I. . M., Zaidan, A. W., Khamirul, A. M., Nurzilla, M., & Halim, S. . A. (2016). Results in Physics Formation , structural and optical characterization of neodymium doped-zinc soda lime silica based glass. *Results in Physics*, *6*, 295–298.

Zhang, B., Chen, Q., Song, L., Li, H., Hou, F., & Zhang, J. (2008). Fabrication and properties of novel low-melting glasses in the ternary system ZnO–Sb_2O_3–P_2O_5. *Journal of Non-Crystalline Solids*, *354*(18), 1948–1954.

Zhang, L., Yin, L., Wang, C., Lun, N., Qi, Y., & Xiang, D. (2010). Origin of visible photoluminescence of ZnO quantum dots: defect-dependent and size-dependent. *The Journal of Physical Chemistry C*, *114*(21), 9651-9658

Zhang, F., Bi, Z., Huang, A., & Xiao, Z. (2015). Luminescence and Judd – Ofelt analysis of the Pr 3 þ doped fluorotellurite glass. *Journal of Luminescence*, *160*(37), 85–89.

Zulfiqar, Yuan, Y., Jiang, Q., Yang, J., Feng, L., Wang, W., Ye, Z., Lu, J. (2016). Variation in luminescence and bandgap of Zn-doped SnO_2 nanoparticles with thermal decomposition. *Journal of Materials Science: Materials in Electronics*. 27(9), 9541-9549.

© COPYRIGHT UPM